



HAL
open science

An engineered extraplastidial pathway for carotenoid biofortification of leaves

Trine Andersen, Briardo Llorente, Luca Morelli, Salvador Torres-montilla, Guillermo Bordanaba-florit, Fausto Espinosa, Maria Rosa Rodriguez-goberna, Narciso Campos, Begoña Olmedilla-alonso, Manuel J. Llansola-Portoles, et al.

► **To cite this version:**

Trine Andersen, Briardo Llorente, Luca Morelli, Salvador Torres-montilla, Guillermo Bordanaba-florit, et al.. An engineered extraplastidial pathway for carotenoid biofortification of leaves. *Plant Biotechnology Journal*, 2021, 19 (5), pp.1008-1021. 10.1111/pbi.13526 . hal-03286028

HAL Id: hal-03286028










<https://hal.science/hal-03286028>

Submitted on 16 Jul 2021

HAL is a multi-disciplinary open access archive for the deposit and dissemination of scientific research documents, whether they are published or not. The documents may come from teaching and research institutions in France or abroad, or from public or private research centers.

L'archive ouverte pluridisciplinaire **HAL**, est destinée au dépôt et à la diffusion de documents scientifiques de niveau recherche, publiés ou non, émanant des établissements d'enseignement et de recherche français ou étrangers, des laboratoires publics ou privés.

An engineered extraplastidial pathway for carotenoid biofortification of leaves

Trine B. Andersen^{1,†} , Briardo Llorente^{1,2,3} , Luca Morelli¹ , Salvador Torres-Montilla¹ , Guillermo Bordanaba-Florit¹, Fausto A. Espinosa¹, Maria Rosa Rodriguez-Goberna¹, Narciso Campos^{1,4} , Begoña Olmedilla-Alonso⁵ , Manuel J. Llansola-Portoles⁶ , Andrew A. Pascal⁶  and Manuel Rodriguez-Concepcion^{1,7,*} 

¹Centre for Research in Agricultural Genomics (CRAG), CSIC-IRTA-UAB-UB, Barcelona, Spain

²Department of Molecular Sciences, ARC Center of Excellence in Synthetic Biology, Macquarie University, Sydney, NSW, Australia

³CSIRO Synthetic Biology Future Science Platform, Sydney, NSW, Australia

⁴Departament de Bioquímica i Biologia Molecular, Universitat de Barcelona, Barcelona, Spain, 08028

⁵Instituto de Ciencia y Tecnología de Alimentos y Nutrición (ICTAN-CSIC), Madrid, Spain

⁶CEA, CNRS, Institute for Integrative Biology of the Cell (I2BC), Université Paris-Saclay, Gif-sur-Yvette, France

⁷Instituto de Biología Molecular y Celular de Plantas (IBMCP), CSIC-Universitat Politècnica de València, Valencia, Spain

Received 2 April 2020;

accepted 9 December 2020.

*Correspondence (Tel (+34) 963 877 725;

fax (+34) 963 877 859; email

manuelrc@ibmcp.upv.es)

†Present address: Great Lakes Bioenergy Research Center, Michigan State University, East Lansing, MI, 48824, USA

Summary

Carotenoids are lipophilic plastidial isoprenoids highly valued as nutrients and natural pigments. A correct balance of chlorophylls and carotenoids is required for photosynthesis and therefore highly regulated, making carotenoid enrichment of green tissues challenging. Here we show that leaf carotenoid levels can be boosted through engineering their biosynthesis outside the chloroplast. Transient expression experiments in *Nicotiana benthamiana* leaves indicated that high extraplastidial production of carotenoids requires an enhanced supply of their isoprenoid precursors in the cytosol, which was achieved using a deregulated form of the main rate-determining enzyme of the mevalonic acid (MVA) pathway. Constructs encoding bacterial enzymes were used to convert these MVA-derived precursors into carotenoid biosynthetic intermediates that do not normally accumulate in leaves, such as phytoene and lycopene. Cytosolic versions of these enzymes produced extraplastidial carotenoids at levels similar to those of total endogenous (i.e. chloroplast) carotenoids. Strategies to enhance the development of endomembrane structures and lipid bodies as potential extraplastidial carotenoid storage systems were not successful to further increase carotenoid contents. Phytoene was found to be more bioaccessible when accumulated outside plastids, whereas lycopene formed cytosolic crystalloids very similar to those found in the chromoplasts of ripe tomatoes. This extraplastidial production of phytoene and lycopene led to an increased antioxidant capacity of leaves. Finally, we demonstrate that our system can be adapted for the biofortification of leafy vegetables such as lettuce.

Keywords: carotenoids, phytoene, lycopene, biosynthesis, *Nicotiana benthamiana*, lettuce, bioaccessibility, antioxidant, biofortification.

Introduction

Carotenoids are lipophilic isoprenoids distributed throughout all kingdoms of life. Plants and some bacteria, archaea and fungi can biosynthesize these compounds *de novo*, whereas the vast majority of animals acquire them through their diet (Rodriguez-Concepcion *et al.*, 2018; Zheng *et al.*, 2020). Carotenoids are an essential part of the human diet, acting as precursors of retinoids (including vitamin A) and health-promoting molecules. They are also economically relevant as natural pigments that provide colours in the yellow to red range to many fruits, vegetables, seafood, fish, poultry and dairy products. One example is lycopene, which gives rise to the red colour in ripe tomatoes. Carotenoids with a shorter conjugation length such as phytoene (the first committed intermediate of the

biosynthetic pathway) are colourless (Rodriguez-Concepcion *et al.*, 2018).

In plants, carotenoids are synthesized in plastids from the universal C5 isoprenoid precursors isopentenyl diphosphate (IPP) and dimethylallyl diphosphate (DMAPP) produced by the methylerythritol 4-phosphate (MEP) pathway (Figure 1). Other plastidial isoprenoids, such as monoterpene and the prenyl moieties of chlorophylls and tocopherols, are produced using the same pool of substrates. In the cytosol, a second pool of IPP and DMAPP is synthesized by the mevalonic acid (MVA) pathway for the production of sesquiterpenoids and triterpenoids (including sterols). Plastid-localized isoforms of geranylgeranyl diphosphate (GGPP) synthases catalyse the condensation of three IPP and one DMAPP into one C20 GGPP. Two GGPP molecules are then converted into one C40 phytoene by phytoene synthase.

Desaturation and isomerization of phytoene produce lycopene, a linear carotenoid whose ends may then be cyclized into β and/or ϵ rings. The formation of two β rings results in the production of β -carotene, from which β - β xanthophylls such as violaxanthin and neoxanthin are formed through oxidation. The formation of one β and one ϵ ring leads to the production of lutein, the most abundant xanthophyll in photosynthetic tissues (Figure 1a). In chloroplasts, carotenoids are involved in light harvesting and photoprotection against excess light, and their levels are finely balanced with those of chlorophylls for the efficient assembly and functionality of photosynthetic complexes (Domonkos *et al.*, 2013; Esteban *et al.*, 2015; Hashimoto *et al.*, 2016). Carotenoids can also be produced and stored at high levels in chromoplasts, which are specialized plastids found in some non-photosynthetic tissues of flowers, fruits and other carotenoid-accumulating tissues (Sadali *et al.*, 2019; Sun *et al.*, 2018).

Several biotechnological strategies have been tested to enrich plant-derived feed and food products with carotenoids to improve their nutritional and economic value (Alos *et al.*, 2016; Zheng *et al.*, 2020). While highly successful results have been obtained in non-photosynthetic tissues, including Golden Rice, manipulation of carotenoid levels in photosynthetic tissues has been much more challenging. We have investigated methods to produce carotenoids in green tissues without interfering with photosynthetic function by moving their biosynthesis away from the chloroplast. The cytosol was a logical choice since the metabolic precursors of carotenoids (IPP and DMAPP) are already present due to the activity of the MVA pathway (Figure 1a). A previous attempt using virus-mediated expression of bacterial enzymes encoding GGPP synthase (*crtE*), phytoene synthase (*crtB*) and a desaturase/isomerase transforming phytoene into lycopene

(*crtI*) resulted in the production of lycopene in the cytosol of tobacco (*Nicotiana tabacum*) cells (Majer *et al.*, 2017). Virus-infected tissues accumulated lycopene to levels up to 10% of the total leaf carotenoid content, but only for 1–2 days, as carotenoid-producing leaves soon became necrotized. Such deleterious phenotype may be caused by side-effects of the viral infection, by the diversion of metabolic substrates away from cytosolic isoprenoid pathways, and/or by negative interference of the lipophilic lycopene with cell membrane function. Here we tested new strategies to circumvent these problems using phytoene and lycopene as the target products. The choice of these carotenoid intermediates (Figure 1a) was based on three main reasons. First, they are virtually absent in non-engineered leaves as they are readily converted into downstream chloroplast carotenoids (Domonkos *et al.*, 2013; Esteban *et al.*, 2015; Hashimoto *et al.*, 2016; Rodriguez-Concepcion *et al.*, 2018). Second, their supply is essential for the eventual production of any downstream carotenoid of interest. And third, they are health-promoting phytonutrients that are only found in a few food sources (Melendez-Martinez *et al.*, 2015; Melendez-Martinez *et al.*, 2018; Müller *et al.*, 2011; Rodriguez-Concepcion *et al.*, 2018).

Results

Agroinfiltrated leaves can produce extrastidial phytoene and lycopene at levels similar to those of endogenous chloroplast carotenoids

To produce phytoene and lycopene in the cytosol without the deleterious effects previously observed using viral vectors (Majer *et al.*, 2017), we tested a combination of strategies using

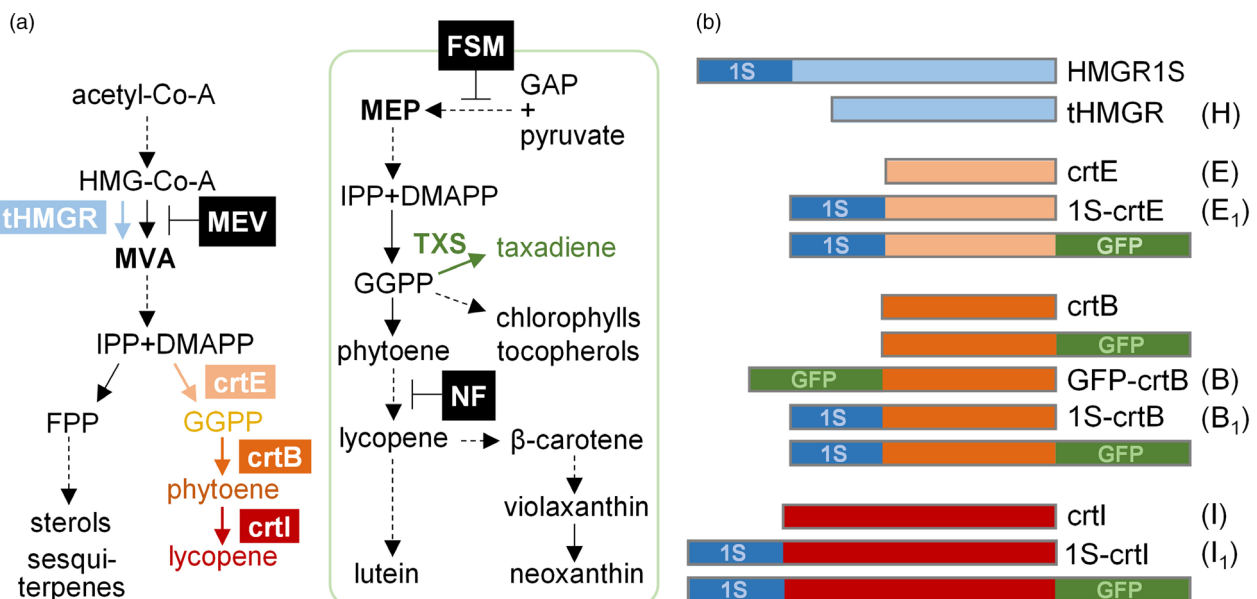
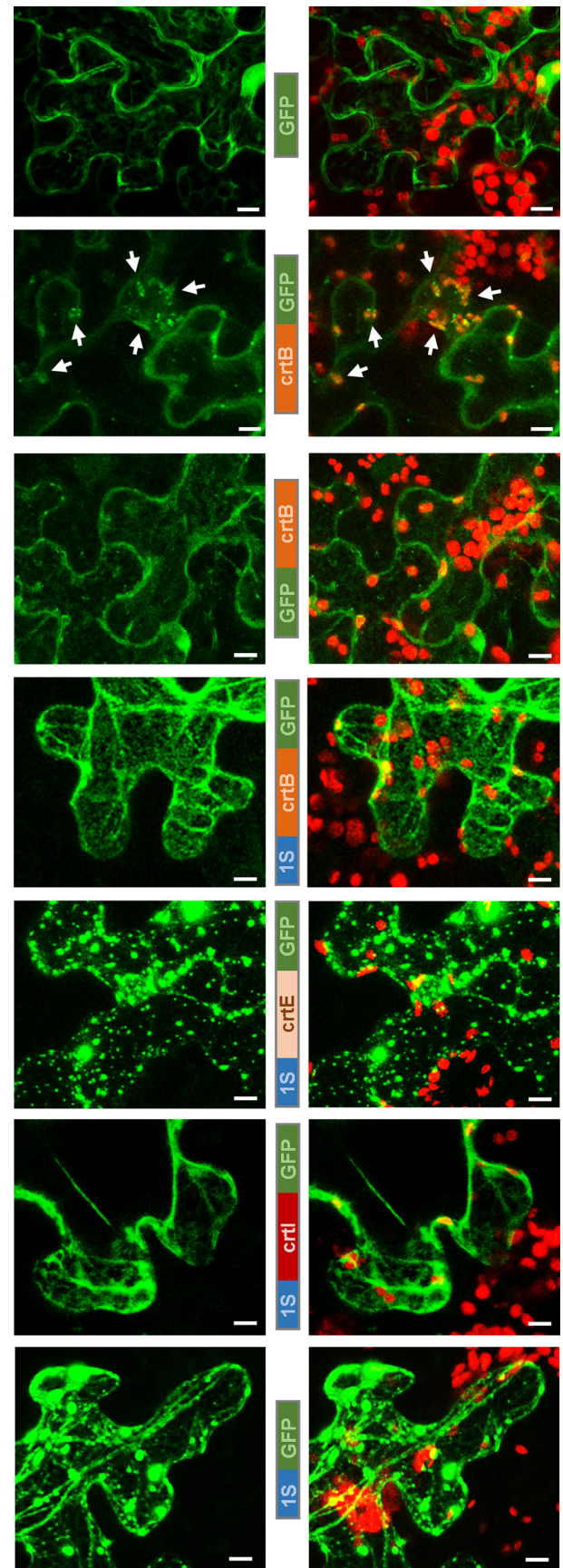


Figure 1 Schematic representation of the pathways and enzymes related to this work. (a) Carotenoid biosynthesis and related isoprenoid pathways in plants. Inhibitors of the MVA pathway (mevinolin, MEV), the MEP pathway (fosmidomycin, FSM) and the carotenoid pathway (norflurazon, NF) are boxed in black. HMG-CoA, hydroxymethylglutaryl coenzyme-A; MVA, mevalonic acid; IPP, isopentenyl diphosphate; DMAPP, dimethylallyl diphosphate; FPP, farnesyl diphosphate; GGPP, geranylgeranyl diphosphate; GAP, glyceraldehyde 3-phosphate; MEP, methylerythritol 4-phosphate. Enzymes produced in our system are shown in colour: tHMGR, truncated HMG-CoA reductase; crtE, bacterial GGPP synthase; crtB, bacterial phytoene synthase; crtI, bacterial desaturase/isomerase; TXS, taxadiene synthase. The green box encloses reactions taking place in plastids. (b) Proteins used in this work. HMGR1S, crtE, crtB and crtI are unmodified enzymes. The rest are either truncated or fusion proteins. Boxes represent different enzymes and tags drawn to scale.

agroinfiltration of *Nicotiana benthamiana* as a less aggressive transient expression system (Schwach *et al.*, 2005). Plasmid vectors expressing the constructs under the control of the constitutive cauliflower mosaic virus 35S promoter together with a plasmid carrying the viral RNA silencing suppressor HCPro were used for transformation of *Agrobacterium tumefaciens* strain GV3101. *N. benthamiana* leaves were infiltrated with *A. tumefaciens* cultures carrying the selected constructs in identical proportions. To convert MVA-derived IPP and DMAPP into carotenoids, the bacterial *Pantoea ananatis* genes encoding crtE (to produce GGPP), crtB (to transform GGPP into phytoene) and crtI (to synthesize lycopene from phytoene) were used (Figure 1a). Unmodified versions of these three bacterial enzymes are active and synthesize lycopene in the cytosol of tobacco leaf cells (Majer *et al.*, 2017). In the case of crtB, however, part of the protein is targeted to chloroplasts (Figure 2) (Llorente *et al.*, 2020). To prevent this, we tested a version of the crtB enzyme with GFP fused to its N-terminus referred to as GFP-crtB (Figure 1b), which is retained in the cytosol of agroinfiltrated *N. benthamiana* leaf cells (Figure 2) (Llorente *et al.*, 2020). When we compared the production of phytoene by crtB and GFP-crtB enzymes at 5 days post-infiltration (dpi) (Figure 3), the amounts were 10-fold higher in the case of the unmodified crtB enzyme. This could be due to the N-terminal GFP tag interfering with crtB activity. Alternatively, the localization of at least some crtB protein in chloroplasts (Figure 2) might involve access to a higher supply of GGPP for phytoene production. Consistent with the latter hypothesis, inhibition of the MEP pathway with fosmidomycin (Figure 1a) strongly decreased the production of phytoene by crtB but not by GFP-crtB (Figure 3a). A similar result was observed when plastidial GGPP levels were decreased by co-expressing a *Taxus baccata* gene encoding taxadiene synthase (Figure 3b), a chloroplast-targeted enzyme that directly converts MEP-derived GGPP into the non-native diterpene taxadiene (Besumbes *et al.*, 2004) (Figure 1a). These results support the conclusion that unmodified crtB produces most of the detected phytoene from plastidial GGPP. In agreement, specific blockage of cytosolic IPP and DMAPP supply with the MVA pathway inhibitor mevinolin (Figure 1a) decreased the production of phytoene by GFP-crtB but not by crtB (Figure 3a). Conversely, increasing cytosolic GGPP levels by co-agroinfiltration of the crtE enzyme resulted in a marginal increment in the production of phytoene by crtB while it doubled the levels of phytoene synthesized by GFP-crtB (Figure 3b). These results indicate that GFP-crtB is enzymatically active and uses MVA-derived GGPP precursors to produce phytoene.

To minimize competition with endogenous cytosolic isoprenoid pathways (Figure 1a), we next increased MVA pathway flux using a truncated version of hydroxymethylglutaryl CoA reductase (HMGR), the main rate-limiting enzyme of the MVA

Figure 2 Subcellular localization of GFP-tagged proteins. *N. benthamiana* leaves were agroinfiltrated with constructs to express the indicated proteins and investigate their subcellular distribution based on GFP fluorescence by confocal microscopy at 3 dpi. Pictures show Z-stacks of selected regions of leaf cells displaying GFP fluorescence either alone (in green; left panels) or in combination with chlorophyll autofluorescence (in red; right panels). Arrows mark chloroplasts showing GFP fluorescence. Scale bars are 10 μ m.



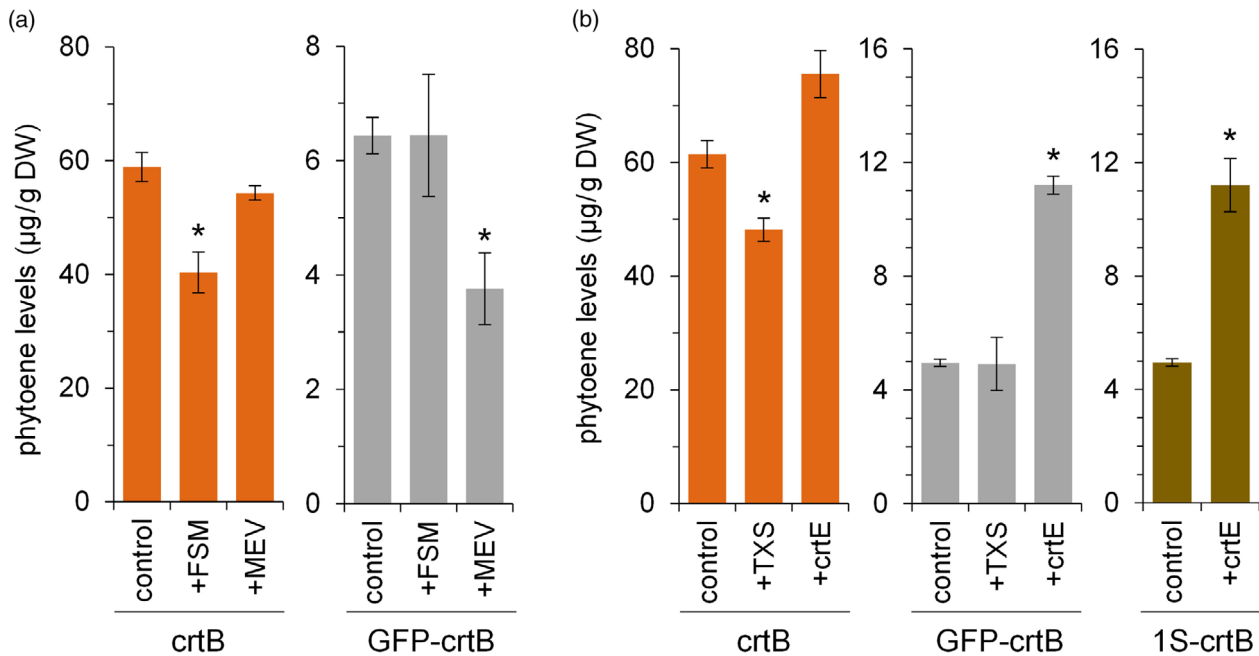


Figure 3 Supply of isoprenoid precursors is limiting for phytoene biosynthesis in the cytosol. *N. benthamiana* leaves were agroinfiltrated with the indicated constructs and samples were collected at 5 dpi for HPLC analysis. (a) Phytoene accumulation in leaf areas expressing either *crtB* or GFP-*crtB*, after treatment with the indicated inhibitors of the MEP or MVA pathways (FSM and MEV, respectively) or a mock solution (control). (b) Phytoene accumulation in leaf areas expressing *crtB*, GFP-*crtB* or 1S-*crtB* either alone (control) or together with yew *TXS* or bacterial *crtE*. Plots show the mean and standard error of $n = 4$ independent samples. Asterisks mark statistically significant changes relative to control samples (t -test, $P < 0.05$).

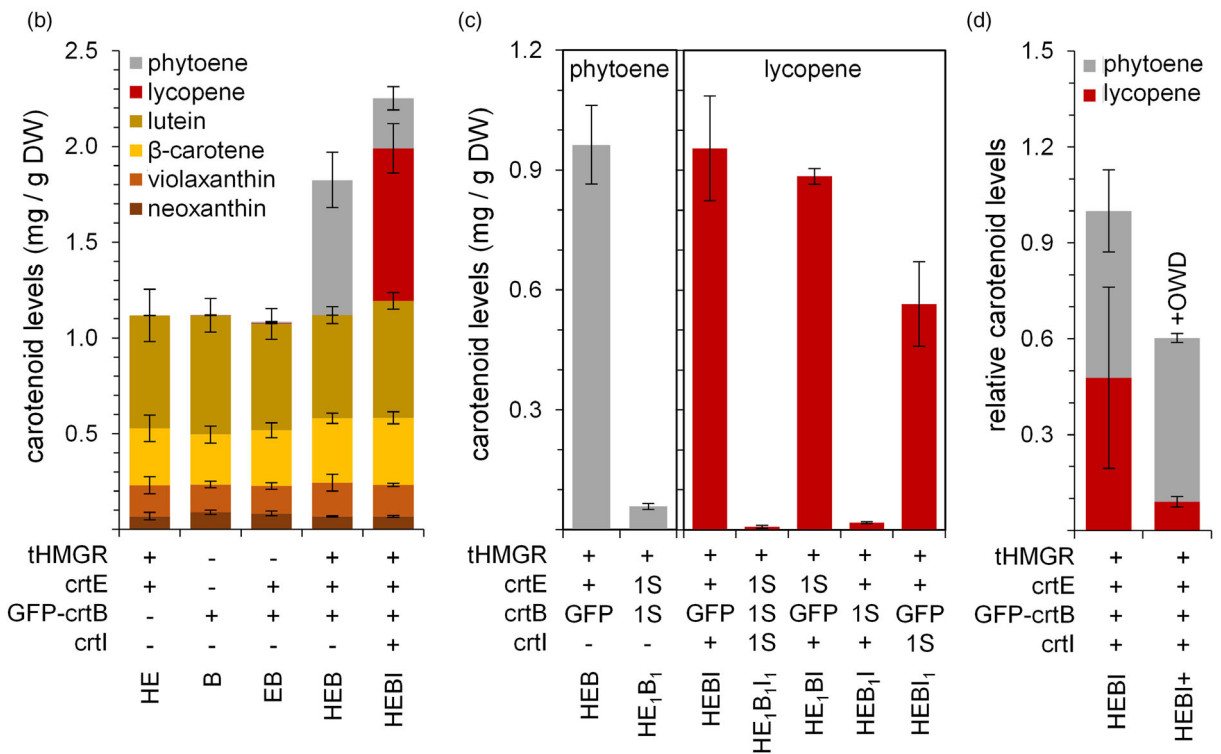
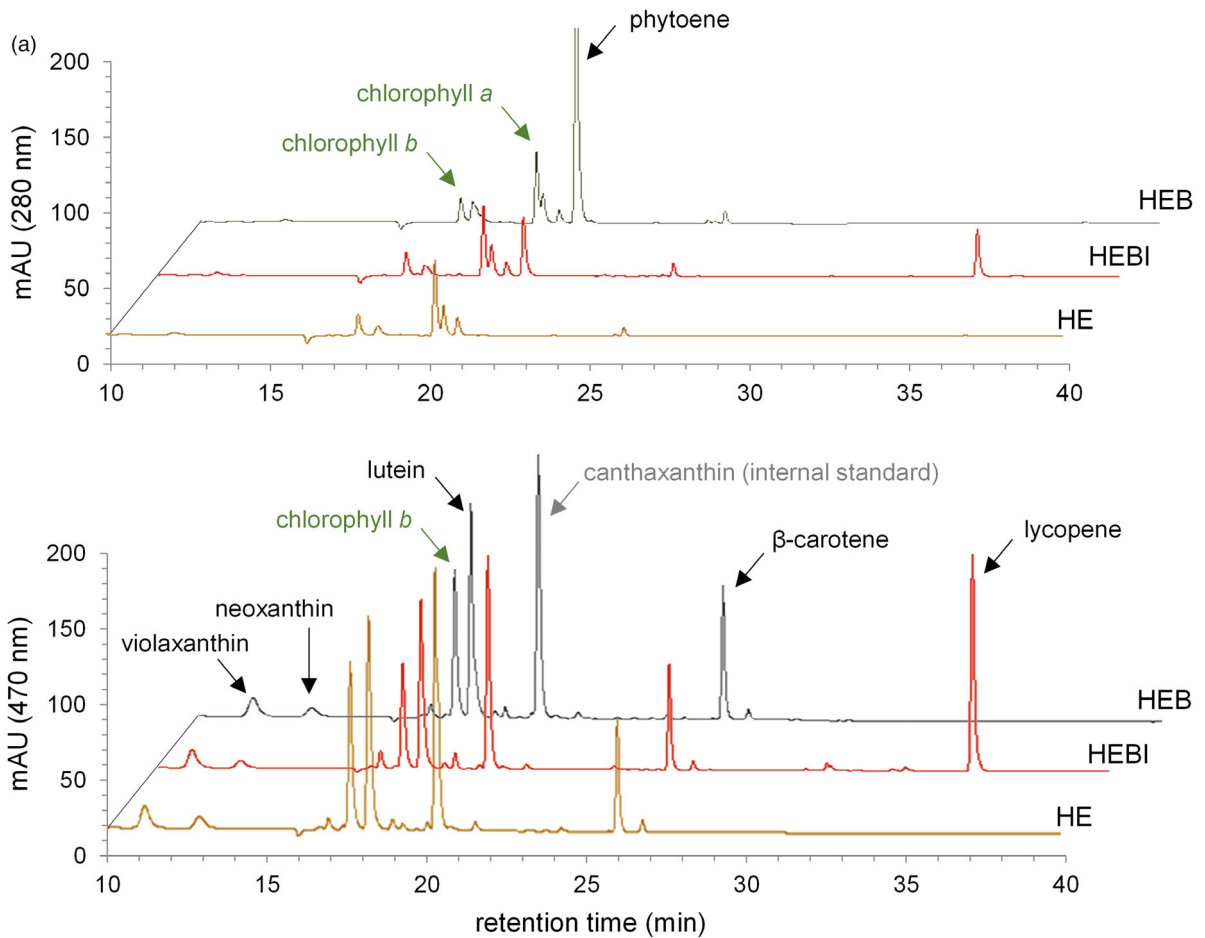
pathway (Rodríguez-Concepción and Boronat, 2015). In particular, we used the *Arabidopsis thaliana* HMGR1 enzyme (At1g76490) lacking the N-terminal regulatory domain (Figure 1b). This truncated version, referred to as tHMGR (Cankar *et al.*, 2015; van Herpen *et al.*, 2010), is not feedback-regulated and localizes to the cytosol as it lacks the N-terminal transmembrane domain that anchors the enzyme to the endoplasmic reticulum (ER). Constructs encoding tHMGR were co-infiltrated with the corresponding bacterial enzymes into *N. benthamiana* leaves and their carotenoid profile was analysed at 5 dpi (Figure 4). Co-agroinfiltration of constructs for tHMGR, *crtE* and GFP-*crtB* (HEB combination) led to an astounding accumulation of phytoene (Figure 4a). While addition of the *crtE* enzyme doubled the production of phytoene compared to GFP-*crtB* alone (EB relative to B, respectively; Figure 3b), a dramatic 200-fold increase in phytoene levels was detected in HEB samples additionally producing tHMGR (Figure 4b). Strikingly, this newly produced cytosolic phytoene increased total carotenoid levels by more than 60%. Further addition of *crtI* (HEBI combination) resulted in the production of very high levels of lycopene but also phytoene, probably reflecting incomplete enzymatic

conversion by *crtI* (Figure 4b). The level of cytosolic carotenoids accumulated in HEBI leaves was similar to the total amount of endogenous chloroplast carotenoids (Figure 4b). In particular, lycopene levels were in the same range of those found in chromoplasts from natural sources specialized for the accumulation of high lycopene levels such as tomato ripe fruit (D'Andrea *et al.*, 2018; Diretto *et al.*, 2020; Flores *et al.*, 2016; Massaretto *et al.*, 2018; Nogueira *et al.*, 2013; Pankratov *et al.*, 2016; Suzuki *et al.*, 2015).

Enhancing the development of endomembrane structures does not improve carotenoid contents

Next, we evaluated the potential of anchoring the bacterial enzymes to cell endomembranes while stimulating the proliferation of such lipid-storage structures to accommodate even higher carotenoid levels without interfering with other cell functions. To do this, we used the N-terminal 178 aa sequence of the *Arabidopsis* HMGR1S isoform. This sequence (named 1S) lacks any catalytic activity, but it includes transmembrane domains for ER membrane anchoring and is sufficient to stimulate a massive proliferation of ER-derived membranes and vesicular

Figure 4 Extrastidial carotenoids are produced at levels similar to those naturally found in chloroplasts. *N. benthamiana* leaf areas agroinfiltrated with different combinations of constructs were collected at 5 dpi for HPLC analysis. (a) HPLC chromatograms of HE, HEB and HEBI samples at 280 nm (to detect phytoene) and 470 nm (to detect coloured carotenoids). The non-plant carotenoid canthaxanthin is used as an internal standard. (b) Levels of carotenoids in leaf areas agroinfiltrated with the indicated combinations. (c) Levels of phytoene and lycopene in leaf areas expressing untagged enzymes (+) or versions with N-terminal GFP or 1S sequences. (d) Levels of phytoene and lycopene in HEBI leaf areas either co-infiltrated or not with a set of three more proteins promoting lipid body formation (indicated as + OWD). Levels are expressed relative to those without OWD. In all cases, plots represent the mean and standard error of $n \geq 3$ independent samples.



structures (Ferrero *et al.*, 2015). Indeed, N-terminal fusion of the 1S sequence to GFP resulted in the localization of the resulting 1S-GFP protein in highly fluorescent bodies corresponding to these proliferating structures (Figure 2). A very similar distribution was observed for 1S-crtE-GFP. In the case of the 1S-crtB-GFP and 1S-crtI-GFP fusions, however, the fluorescent bodies were not observed and the proteins localized only in ER membranes (Figure 2).

The combination tHMGR, 1S-crtE and 1S-crtB (HE₁B₁) produced 0.06 mg of phytoene per g of DW (or 60 µg/g DW), which is about 15-fold lower than that produced by the HEB samples (Figure 4c) but fivefold higher than that produced by crtE and 1S-crtB (Figure 3b). These results suggest that the addition of the 1S domain to crtB or crtE does not block their enzymatic activity, but rather inhibits correct use of the extra MVA-derived precursors that result from tHMGR activity. Consistent with this interpretation, when tHMGR and 1S-fused crtE, crtB and crtI enzymes were used (HE₁B₁ combination), the production of lycopene showed a dramatic drop (Figure 4c). By using only one of the three bacterial enzymes fused to 1S, however, different effects were observed. The use of 1S-crtE did not have a significant impact compared to crtE, but a reduction occurred when crtI was substituted with 1S-crtI, and a major inhibition resulted from using 1S-crtB in place of GFP-crtB (Figure 4c).

As an alternative strategy to improve carotenoid storage in extrastidial compartments, we next stimulated the proliferation of oleosin-coated lipid bodies. The strategy, based on the agroinfiltration of sequences encoding oleosins, diacylglycerol acyltransferase, and the transcription factor WRINKL1, has recently been reported as contributing successfully to the storage of lipophilic MVA-derived sesquiterpenes (Figure 1a) in *N. benthamiana* leaves (Delatte *et al.*, 2018). Addition of the plasmids encoding these proteins to the HEBI mix, however, was detrimental to lycopene accumulation and neutral for phytoene (Figure 4d).

Extrastidial phytoene and lycopene accumulation eventually reduce chlorophyll contents and photosynthetic activity

The massive levels of lycopene that accumulated in *N. benthamiana* leaves agroinfiltrated with HEBI constructs resulted in a characteristic red colour in the sectors that produced the pigment (Figure 5). By contrast, HEB areas producing only phytoene were visually indistinguishable from agroinfiltrated control HE areas, as expected due to the colourless nature of phytoene (Figure 5a). At the cell level, tubular structures of distinctive red colour were observed inside HEBI cells (Figure 5b), suggesting that they might correspond to lycopene crystals. The red colour of lycopene-accumulating areas was stable for about a week and then it gradually faded. Leaf pigmentation actually paralleled the accumulation profile of lycopene, which steadily increased to 5 dpi, and then remained high for at least two more days (Figure 5c). Interestingly, the levels of endogenous (i.e. chloroplastidial) carotenoids in HEBI leaves remained unchanged, whereas chlorophyll levels started to decrease at 5 dpi and by 7 dpi they had dropped about 20% (Figure 5c). Phytoene production in *N. benthamiana* leaves agroinfiltrated with HEB constructs appeared to be still active at 7 dpi (Figure 5c). Similar to lycopene-producing HEBI leaf tissues, HEB areas accumulating cytosolic phytoene showed a decrease in chlorophyll levels and no changes in chloroplast-associated carotenoids. In this case, however, the reduction in chlorophyll contents occurred later (at 7 dpi) and to a

lower degree (10%) compared to lycopene-producing HEBI leaf tissues (Figure 5c). No changes in carotenoid or chlorophyll levels were observed in control HE leaves (Figure 5c), suggesting that the decrease in chlorophyll levels observed in leaves producing phytoene and lycopene is not due to the agroinfiltration procedure but to the accumulation of those carotenoids outside chloroplasts. Analysis of chloroplast ultrastructure by transmission electron microscopy (TEM) of leaf cells at 7 dpi showed a higher abundance of plastoglobules in HEB chloroplasts compared to HE controls (Figure 5d). The development of plastoglobules was more evident in HEBI chloroplasts, which also showed a decreased abundance of thylakoid membranes and grana (Figure 5d).

To check whether the changes in leaf chlorophyll levels and chloroplast ultrastructure caused by extrastidial accumulation of phytoene and lycopene had any impact on photosynthesis, we next quantified effective quantum yield of photosystem II (ϕPSII) at different time points after agroinfiltration with HE, HEB or HEBI combinations (Figure 5e). Phytoene-producing HEB leaves only showed a statistically significant decrease in the ϕPSII value at 7 dpi, whereas HEBI tissues producing lycopene showed a stronger reduction even at earlier time points (Figure 5e). While our results demonstrate that leaf cells remain photosynthetically active despite accumulating phytoene and lycopene at levels similar to those of photosynthesis-related chloroplast carotenoids (i.e. lutein, β-carotene, violaxanthin and neoxanthin), they also show that chloroplast features are altered by the accumulation of phytoene and, particularly, lycopene in extrastidial locations.

Phytoene shows improved bioaccessibility when accumulated outside plastids

Phytoene is a health-promoting carotenoid naturally found in some non-green fruits and vegetables such as tomatoes but normally absent from leaves (Melendez-Martinez *et al.*, 2015; Melendez-Martinez *et al.*, 2018). The accumulation of phytoene in HEB leaves reached levels of ca. 1 mg/g DW, similar or even higher than those found in ripe tomatoes (D'Andrea *et al.*, 2018; Dretto *et al.*, 2020; Flores *et al.*, 2016; Massaretto *et al.*, 2018; Nogueira *et al.*, 2013; Pankratov *et al.*, 2016; Suzuki *et al.*, 2015). However, it was unknown whether the subcellular localization of phytoene might impact its bioaccessibility (i.e. the quantity released from the plant matrix in the gastrointestinal tract that becomes available for absorption and eventual biological activity). To address this question, we compared bioaccessibility of extrastidial phytoene from agroinfiltrated HEB leaves and plastidial phytoene from non-infiltrated leaves treated with norflurazon (NF), an inhibitor of phytoene desaturation (Figure 1a). *N. benthamiana* leaves were infiltrated either with *A. tumefaciens* cultures carrying the HEB constructs or with NF and collected 5 days later. Non-infiltrated leaves were also collected as a control, and tissue from all samples was freeze-dried and ground to a fine powder that was used for both HPLC and *in vitro* digestion assays (Figure 6). HPLC analysis of the samples showed that the NF treatment resulted in the accumulation of some phytoene and only caused a slight reduction in the levels of downstream carotenoids compared to control leaves (Figure 6a). The levels of phytoene in HEB leaf samples were much higher than those in NF-treated samples, whereas the amount of chloroplast carotenoids remained unchanged compared to control leaves (Figure 6a). To facilitate bioaccessibility comparisons, we mixed 1 volume of lyophilized HEB tissue with 5 volumes of

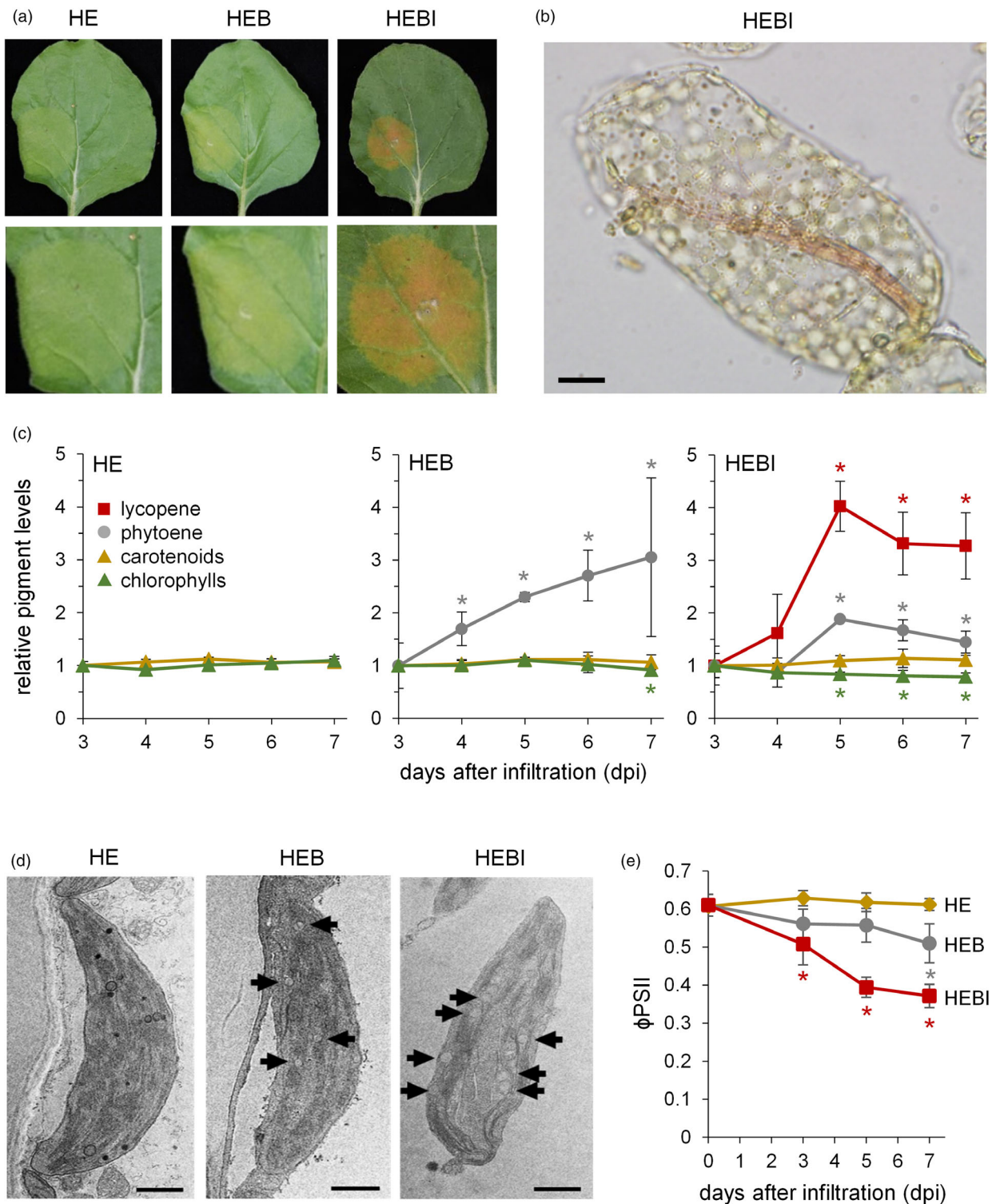


Figure 5 Accumulation of extraplasmidial phytoene and lycopene indirectly impacts photosynthesis. (a) Representative pictures of *N. benthamiana* leaves agroinfiltrated in their lower left-hand side with constructs to express HE, HEB and HEBI combinations. The lower panels show a magnification of the agroinfiltrated areas. (b) Picture of a leaf cell from a HEBI-infiltrated area. Note the distinctive red tubular structure within the cell, likely to be a large lycopene crystal. Scale bar is 10 μm . (c) Photosynthetic pigment levels in HE, HEB and HEBI leaf areas at the indicated times after agroinfiltration. Carotenoid contents refer to endogenous (i.e. chloroplastic) species, excluding phytoene and lycopene. Values are the mean and standard error of $n \geq 3$ independent samples relative to levels at 3 dpi. Asterisks mark statistically significant changes (t -test, $P < 0.05$) relative to 3 dpi. (d) TEM images of representative chloroplasts from leaf areas like those shown in (a) at 7 dpi. Arrows mark plastoglobules in HEB and HEBI chloroplasts. Scale bars are 1 μm . (e) Effective quantum yield of PSII (ϕPSII) in leaf sections agroinfiltrated with the indicated combinations. Plots represent the mean and standard error of $n \geq 3$ independent samples. Asterisks mark statistically significant changes (t -test, $P < 0.05$) relative to 0 dpi.

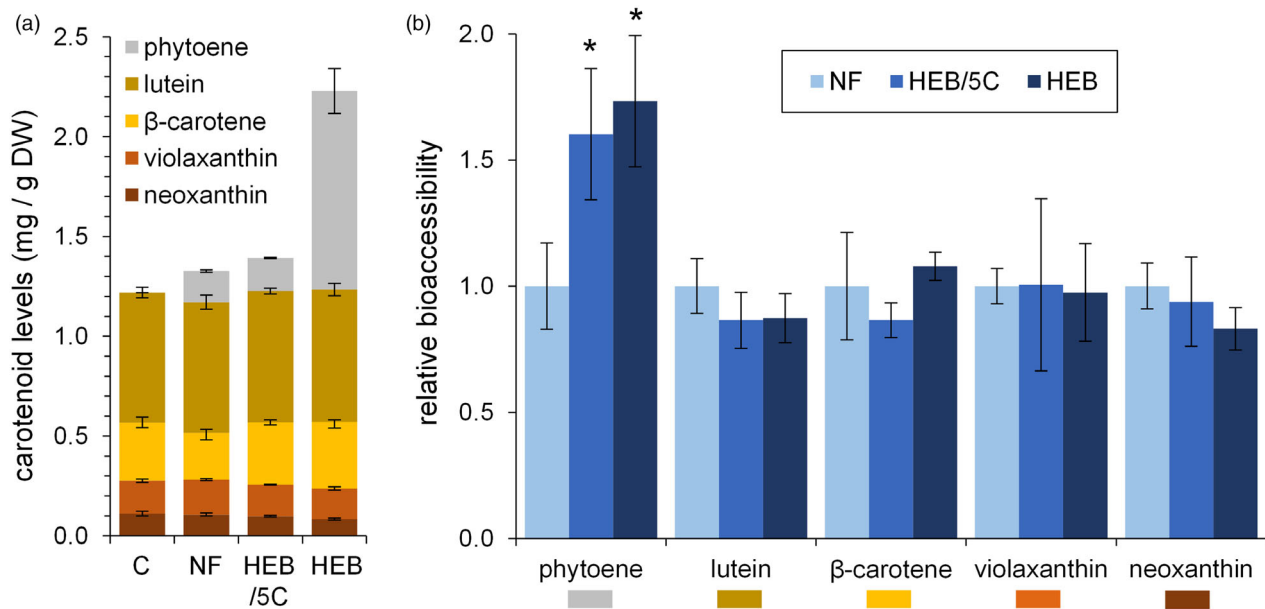


Figure 6 Bioaccessibility of phytoene changes depending on its subcellular accumulation site. *N. benthamiana* leaves were agroinfiltrated with HEB constructs to produce extrastidial phytoene or treated with norflurazon (NF) to accumulate phytoene inside chloroplasts and collected 5 days later. Non-infiltrated, untreated leaves were collected at the same time as a control (sample C). Freeze-dried tissue from these leaf samples was ground and used for both for HPLC and bioaccessibility analysis. A sample combining one part of HEB and five parts of C ground tissue (named HEB/5C) was also used for experiments. (a) HPLC analysis of carotenoids in the indicated samples. (b) Bioaccessibility of the carotenoids shown in (a). Values correspond to the mean and standard error of $n = 3$ independent samples per treatment represented relative to those of NF-treated leaves. Asterisks mark statistically significant changes relative to NF-treated samples (t -test, $P < 0.05$).

control tissue to create a new sample (named HEB/5C) with levels of extrastidial phytoene similar to the plastidial phytoene contents of NF samples (Figure 6a). Then, a standardized *in vitro* method that simulates digestion was used to estimate the bioaccessibility of phytoene in leaves when accumulated either inside or outside plastids (NF-treated leaves or HEB and HEB/5C samples, respectively). Using this *in vitro* method, which reproduces physiological conditions *in vivo* by using specific digestive enzymes under conditions mimicking oral, gastric and small intestinal digestion phases, bioaccessibility of phytoene was found to be 60–70% higher in HEB and HEB/5C samples compared to NF-treated leaves (Figure 6b). By contrast, bioaccessibility of the endogenous (chloroplast) carotenoids was similar in all the samples (Figure 6b). The results support the conclusion that extrastidial accumulation improves phytoene bioaccessibility.

Cytosolic lycopene crystals in leaves are similar to those present in tomato fruit chromoplasts and contribute to increase antioxidant capacity

Like phytoene, lycopene is associated with health benefits but its bioaccessibility is much lower in part because lycopene-rich products such as a ripe tomato fruits accumulate this carotenoid as intrastidial crystals (Cooperstone *et al.*, 2015; Mapelli-Brahm *et al.*, 2018). To test whether the tubular structures that were visible in HEBI cells (Figure 5b) correspond to lycopene crystalloids, we initially recorded the absorption spectra of *N. benthamiana* HE, HEB and HEBI leaves and then calculated the difference spectra for HEB-minus-HE and HEBI-minus-HE (Figure 7a). The HEBI-HE difference spectrum exhibited two peaks in the carotenoid region at 528 and 568 nm, that were absent in

the HEB-HE spectrum. This indicates the presence of a new carotenoid species absorbing in this region in HEBI. The peaks are coincident with the 0-1 and 0-0 vibronic transitions, respectively, reported for lycopene crystalloids in tomatoes (Ishigaki *et al.*, 2017; Llansola-Portoles *et al.*, 2018). To analyse the features of the HEBI lycopene crystals further, we turned to resonance Raman spectroscopy, a technique that provides rich information about the vibrational properties of carotenoids. The vibrational modes in the ν_7 region, around 1520 cm^{-1} , arise from stretching vibrations of the double bonds of the linear carotenoid skeleton (Koyama and Fujii, 1999; Robert, 1999). Resonance Raman spectra at 77 K upon 514.5 and 577 nm excitation were recorded for HEBI and control HE leaves, and compared with that of ripe tomatoes (Figure 7b). At 514.5 nm, both HE and HEBI leaves exhibit a wide ν_7 mode but with somewhat shifted maxima – 1525.8 cm^{-1} in HE and 1523.8 cm^{-1} in HEBI. An even lower frequency is observed in the case of ripe tomato fruit (peak at 1521.5 cm^{-1} ; Figure 7b), as previously described (Llansola-Portoles *et al.*, 2018). HE samples excited at 577 nm exhibited a wide vibrational mode, peaking at the same frequency as at 514.5 nm (1525.8 cm^{-1}). In contrast, the ν_7 mode for HEBI at 577 nm is significantly narrower and down-shifted to 1513.1 cm^{-1} , overlapping with the spectrum of tomatoes at this wavelength (Figure 7b). Note that the signals recorded in leaves for 577 nm excitation are very noisy, as they overlap with the blue tail of the large chlorophyll fluorescence signal. Taken together, these data indicate that HEBI leaves exhibit contributions both from chloroplast carotenoids and from a new red-absorbing species. This red-shifted carotenoid dominates the spectrum at 577 nm, as it is in pre-resonance with its 0-0 absorption transition at 568 nm (see above) giving a narrow ν_7 contribution at 1513.1 cm^{-1} , as

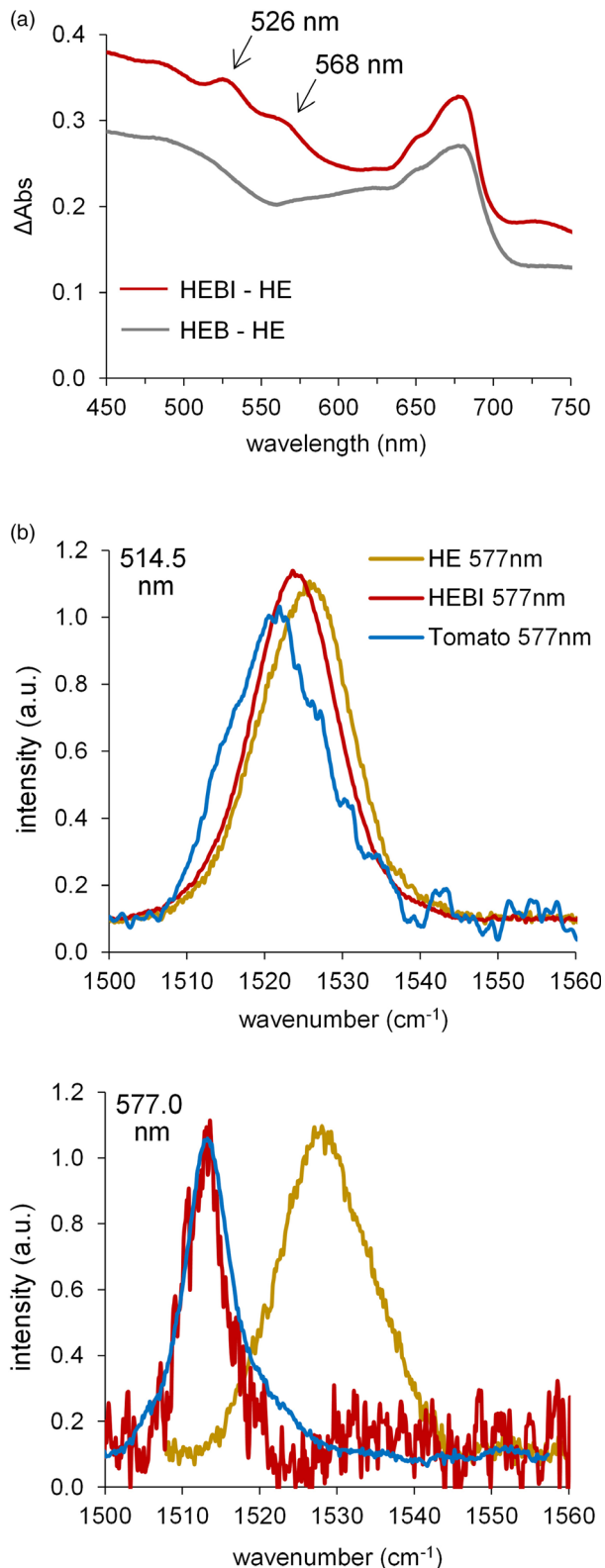


Figure 7 Lycopene crystalloids in HEBI leaves are similar to those in tomato fruit chromoplasts. (a) Absorption difference spectra of *N. benthamiana* leaves (HEB and HEBI-minus-HE) obtained at room temperature in reflectance mode. (b) 77 K resonance Raman spectra in the ν_7 region for *N. benthamiana* HE and HEBI leaves and red (ripe) tomato fruit at 514.5 and 577 nm excitation.

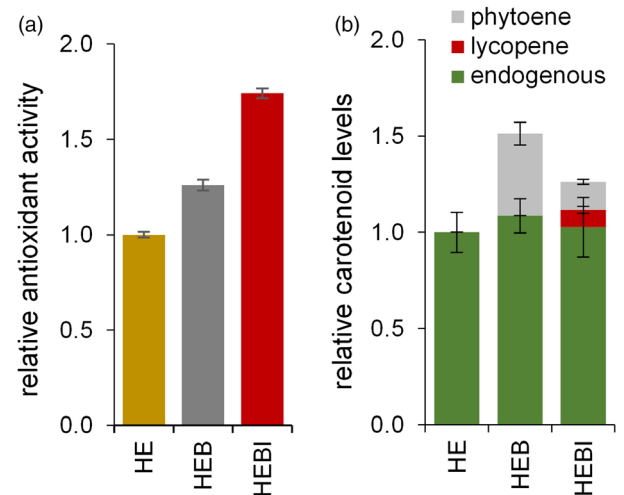


Figure 8 Cytosolic production of phytoene and lycopene contribute to biofortification. (a) Antioxidant capacity of *N. benthamiana* HE, HEB and HEBI leaves. Values correspond to the mean and standard error of $n = 3$ independent samples represented relative to those of control (HE) leaves. (b) Levels of carotenoids in lettuce leaves agroinfiltrated with the indicated combinations of constructs. Mean and standard error of $n \geq 4$ independent samples are represented relative to those in HE leaves.

observed in tomatoes. A mixture of both carotenoid populations (new red species and chloroplast carotenoids) is observed when exciting HEBI at 514.5 nm, as this wavelength is midway between the newly observed 0-1 band (528 nm) and the 0-0 transitions of photosynthetic carotenoids (~ 500 nm and below). In this case, ν_7 exhibits a frequency intermediate between 1513.1 cm^{-1} (red species) and 1525.8 cm^{-1} (chloroplast carotenoids; see HEB at this wavelength). The marked similarity between the extraplastidial lycopene crystals formed in HEBI leaves and the lycopene crystalloids naturally present in ripe tomatoes, in terms of their vibrational and electronic properties, indicates a very similar organization and aggregation state in both cases.

Lycopene is a major contributor to the antioxidant properties of carotenoid-containing foods (Müller *et al.*, 2011). In agreement, the accumulation of lycopene in HEBI leaves resulted in an astounding 80% increase in antioxidant activity of the leaf tissue as determined using the Trolox equivalent antioxidant capacity (TEAC) test (Figure 8a). Also consistent with the much lower antioxidant capacity of phytoene (Müller *et al.*, 2011), the TEAC value of phytoene-producing HEB leaves was only 30% higher than that of HE controls (Figure 8a).

Cytosolic carotenoid production in edible lettuce leaves

Our strategy of engineering a synthetic cytosolic pathway to boost carotenoid levels in green (i.e. chloroplast-containing) tissues could be readily applied to the biofortification of edible leafy vegetables. As a proof of concept, we tested whether agroinfiltration could also work to transiently express the required genes in romaine lettuce (*Lactuca sativa*), a widely consumed and inexpensive salad vegetable with a relatively low nutritional value (Mou, 2009). Lettuce leaves were found to be more difficult to agroinfiltrate than those of *N. benthamiana*, but vacuum agroinfiltration was successful in transiently expressing HEB and HEBI combinations leading to extraplastidial phytoene and/or lycopene overproduction in some leaf areas (Figure 8b). The levels of total

carotenoids (i.e. extraplasmidial and chloroplastic) were clearly enhanced in agroinfiltrated areas, although the accumulation of phytoene and/or lycopene was lower than that achieved in *N. benthamiana*.

Discussion

In this paper, we show that carotenoids can be produced and accumulated in very high amounts for over a week in the cytosol of leaf cells. We demonstrate major improvements compared to our first attempts in *N. tabacum* using viral vectors carrying untagged crtE, crtB and crtI enzymes (Majer *et al.*, 2017). First, agroinfiltration of *N. benthamiana* leaves was found to be a much faster and reliable method to test enzyme combinations with minimal interference from chlorosis and necrosis. Second, using the GFP-crtB protein ensured cytosolic localization of the phytoene-producing crtB enzyme (Llorente *et al.*, 2020). Third, adding a deregulated version of the HMGR enzyme (tHMGR) boosted cytosolic GGPP supply to reach much higher phytoene and lycopene levels than those achieved in our previous work. Fourth, extraplasmidial carotenoid levels remained high for much longer than when using viral vectors. And fifth, we showed that the accumulation of these extraplasmidial carotenoids provides nutritional benefits that can be transferred to leafy vegetables such as lettuce, hence demonstrating the feasibility of using this strategy for food biofortification.

Rapid testing of different gene combinations by agroinfiltration led to establish that a major limiting step for carotenoid biosynthesis outside plastids was the supply of their metabolic precursors (Figure 3). To enhance the production of these precursors, we used a truncated form of HMGR, considered to be the main rate-determining enzyme of the MVA pathway (Rodríguez-Concepción and Boronat, 2015). This truncated form (tHMGR) retains the cytosolic domain bearing its catalytic activity but lacks the N-terminal 1S region required to anchor the enzyme to the ER (Figure 1). As the N-terminal region is also key for the regulation of HMGR enzyme levels and activity, the tHMGR protein is a deregulated and more stable version of the enzyme (Doblas *et al.*, 2013; Leivar *et al.*, 2011; Pollier *et al.*, 2013; Rodríguez-Concepción and Boronat, 2015). The use of tHMGR enzymes has already been shown to increase the production of MVA-derived isoprenoids such as sesquiterpenes and sterols (Figure 1) (Andersen *et al.*, 2017; Cankar *et al.*, 2015; Chappell *et al.*, 1995; Harker *et al.*, 2003; van Herpen *et al.*, 2010; Lee *et al.*, 2019; Wu *et al.*, 2006; Yin and Wong, 2019). The highest increases have been typically obtained in transient expression assays with *N. benthamiana* leaves similar to those used in our work. In particular, addition of *Arabidopsis* tHMGR to agroinfiltrated gene combinations caused a 37-fold increase in endogenous sesquiterpenes levels (Cankar *et al.*, 2015) and boosted the production of exogenous sesquiterpenes (i.e. those not naturally found in *N. benthamiana*) up to 300-fold (van Herpen *et al.*, 2010). The ca. 100-fold increase in phytoene levels observed after incorporating tHMGR with the combination of GFP-crtB and crtE (i.e. HEB vs. EB; Figures 3b and 4b) falls within the same range.

Unlike sesquiterpenoids, carotenoids such as phytoene and lycopene are not naturally produced in the cytosol of plant cells. We therefore reasoned that the levels of carotenoids accumulated outside plastids could be further increased by improving the capacity of leaf cells to sequester and store these lipophilic isoprenoids through the development of ER-derived membrane systems and lipid bodies. Fusion of the 1S domain of the

Arabidopsis HMGR1S isoform to crtE successfully targeted the resulting enzyme to the ER, and also stimulated a massive development of ER-derived membranes and vesicular structures similar to those observed with the 1S-GFP protein (Figure 2) (Ferrero *et al.*, 2015). In the case of crtB and crtI, however, the proteins 1S-crtB-GFP and 1S-crtI-GFP were targeted to the ER membranes but did not stimulate the proliferation of fluorescent bodies (Figure 2), perhaps because they were produced at lower levels than the 1S-crtE-GFP fusion. Consistently, the number of cells showing detectable GFP fluorescence was much lower in leaf areas agroinfiltrated with 1S-crtB-GFP or 1S-crtI-GFP compared to those agroinfiltrated with 1S-crtE-GFP or 1S-GFP. In addition, the fusion to 1S did not have a substantial impact on crtE activity (i.e. in the production of GGPP) but it dramatically prevented the conversion of GGPP into phytoene and had a negative impact on the synthesis of lycopene from phytoene (Figure 4c). It is possible that cytosolic (i.e. soluble) GFP-crtB and crtI enzymes could associate for efficient channelling of GGPP provided by either soluble or membrane-bound crtE to lycopene, which would then be released to form crystals. Indeed, it has been suggested that these bacterial enzymes might interact to form a multiprotein complex and/or create a microenvironment to function as a metabolon for efficient substrate channelling when produced inside plastids (Nogueira *et al.*, 2013; Ravanello *et al.*, 2003). ER-membrane association might prevent such direct interaction of the enzymes, negatively impacting lycopene production. The observation that ER-targeting of crtB results in a dramatic block of phytoene production in samples containing soluble tHMGR (Figure 4c) but not in those harbouring only the endogenous ER-anchored HMGR enzymes (Figure 3b) further supports the conclusion that high phytoene (and lycopene) titres require a completely soluble synthetic pathway for efficient metabolite channelling.

Another remarkable observation of our work was that proliferation of ER-derived membrane structures (e.g. in leaf areas expressing 1S-crtE) or lipid bodies did not provide an advantage for the accumulation of extraplasmidial carotenoids (Figure 4). This might not be so surprising in the case of lycopene, which was later found to form cytosolic crystals (Figure 7). It is likely, however, that lycopene produced in HEBI leaves is initially stored in association with cell membranes before reaching a concentration high enough to crystallize. In the case of phytoene, fruits that produce high amounts of this carotenoid store it in lipophilic vesicles inside chromoplasts that are sometimes released into the cytosol, probably to remove excess amounts accumulated in plastidial membranes (Lado *et al.*, 2015; Nogueira *et al.*, 2013). Whether the massive amounts of phytoene produced in HEB and HEBI cells are sequestered in cell membrane systems other than those derived from the ER (e.g. vacuoles or plasma membrane) remains unknown. However, the observation that the bioaccessibility of phytoene produced in HEB leaves is significantly higher than that accumulated in the plastids of NF-treated leaves (Figure 6b) suggests that phytoene might be less tightly associated to membranes when produced and stored at extraplasmidial locations.

Regardless of the storage mechanism, the accumulation of extraplasmidial carotenoids in our system achieved levels comparable to those of endogenous chloroplast carotenoids and, significantly, these levels remained high for over a week. This represents a dramatic increase in stability relative to our previous results using viral vectors, when lycopene levels dropped soon after the leaves exhibited a red colour (Majer *et al.*, 2017). It is

possible that crystallization of lycopene in HEBI leaves after reaching levels similar to those found in tomato fruit chromoplasts could contribute to its higher stability, as crystals are metabolically and osmotically inert and probably less prone to oxidative or enzymatic degradation. Nevertheless, the formation of cytosolic lycopene crystals in HEBI cells and the accumulation of similarly high levels of phytoene in HEB cells had a negative effect on cell fitness. Indeed, several signs of cell damage, including chlorosis and eventual necrosis, developed about a week after agroinfiltration in HEB and HEBI leaves. The reduction in chlorophyll levels, the increased number of chloroplast plastoglobules, the decreased abundance of thylakoids and grana, and the defects in photosynthetic activity detected in these leaves (Figure 5) strongly suggest that extraplastidial accumulation of lycopene and, to a lesser extent, phytoene triggered a leaf senescence process. Indeed, the earliest changes associated with leaf senescence occur in the chloroplast and cause chlorosis before necrotic symptoms are observed (Tamary et al., 2019). It seems likely that these deleterious, senescence-like effects observed in HEB and HEBI leaves might be related to cell damage caused by the disruption of normal cell compartments, functions and/or metabolism upon accumulation of extraplastidial isoprenoids. Alternatively, signals derived from the cleavage of cytosolic phytoene, lycopene or intermediate carotenoid species might be transduced to regulate chloroplast structure and function, including photosynthetic activity (Avendano-Vazquez et al., 2014; Cazzonelli et al., 2020).

Very little attention has been paid to carotenoid biofortification of green vegetables to date, in part because of the challenges associated with changing the balance between carotenoids and chlorophylls (Alos et al., 2016; Domonkos et al., 2013; Esteban et al., 2015; Hashimoto et al., 2016; Zheng et al., 2020). Nonetheless, recent reports have shown that *N. benthamiana* leaves overexpressing regulators of carotenoid gene expression and storage were able to double their carotenoid content in chloroplasts (Ampomah-Dwamena et al., 2019; D'Amelia et al., 2019; Llorente et al., 2020; Wang et al., 2018). Here we report a similar twofold increase in total carotenoid levels in *N. benthamiana* leaves (Figure 4b). Despite the defects on cell function described above, our system for cytosolic production of carotenoids offers multiple advantages over those modifying the plastidial carotenoid content. Firstly, the composition of chloroplast carotenoids remains unchanged in our system (Figure 5c) and therefore their photosynthetic and photoprotective functions are not directly impacted. Although a likely secondary cell damage-associated effect does cause photosynthesis to slow down (Figure 5e), it is not blocked and can therefore continue to support plant growth while the extraplastidial carotenoids are produced and stored. Secondly, our system separates the carotenoid intermediates from those plastidial enzymes that convert them into downstream products or degrade them into cleavage products, including apocarotenoid signals (Rodriguez-Concepcion et al., 2018). While non-enzymatic degradation could still occur, it does not appear to be a problem to achieve high titres of extraplastidial carotenoids in our system. Together with the unexpected capacity of leaf cells to accumulate carotenoids outside chloroplasts, this resulted in levels of phytoene and lycopene up to 1 mg/g DW, in the range of those found in chromoplasts from natural sources such as ripe tomato fruit (D'Andrea et al., 2018; Diretto et al., 2020; Flores et al., 2016; Massaretto et al., 2018; Nogueira et al., 2013; Pankratov et al., 2016; Suzuki et al., 2015). Thirdly, the system is very

flexible, and the incorporation of additional enzymes catalysing downstream steps is feasible so that a much broader variety of carotenoids could be produced (Nogueira et al., 2019). Finally, we demonstrate that this system can be adapted to the bioengineering of leafy vegetables such as lettuce, improving their antioxidant capacity, bioaccessibility and overall nutritional quality.

N. benthamiana is particularly well suited to produce high titres of valuable enzymes and metabolites for molecular pharming due to a fast growth rate and a natural ability to express heterologous gene sequences, among other traits (Lomonosoff and D'Aoust, 2016). While agroinfiltration assays can be scaled up for industrial production of carotenoids and other metabolites in *N. benthamiana*, adaptation to crops such as lettuce for human or animal consumption should require further efforts in the development and optimization of safe and reliable transient expression methods with no health risks. Stable expression of transgenes appears as a valid alternative from the technical point of view. However, the poor consumer acceptance of transgenesis has turned the attention to genome editing. New varieties of leafy food (e.g. lettuce, spinach, cabbage, kale, chard) and forage crops (e.g. alfalfa, grasses) could be generated by editing endogenous genes to overaccumulate carotenoids in extraplastidial locations. Flux-controlling enzymes involved in isoprenoid biosynthesis (including HMGR, GGPP synthase and phytoene synthase) are encoded by small gene families in most plants. In the case of GGPP synthase, cytosolic isoforms are naturally present (Ruiz-Sola et al., 2016). For the rest, CRISPR-Cas9 technology could be used to remove the N-terminal region from non-essential and/or tissue-specific isoforms of HMGR (to create truncated forms similar to the tHMGR version used here) and carotenoid biosynthetic enzymes such as phytoene synthase (to remove the plastid transit peptide and create a cytosolic version). Furthermore, our results open the door to the biofortification of leafy vegetables with other health-promoting isoprenoids such as tocopherols (vitamin E), phylloquinones (vitamin K1) and plastoquinone by engineering extraplastidial biosynthetic pathways using MVA-derived precursors.

Methods

Plant material, growth conditions and treatments

Nicotiana benthamiana RDR6i, tomato (*Solanum lycopersicum*) MicroTom and lettuce (*Lactuca sativa*) Romaine plants were grown in a greenhouse under standard long-day conditions as described (D'Andrea et al., 2018; Llorente et al., 2016; Majer et al., 2017). For *N. benthamiana* agroinfiltration, the second or third youngest leaves of 4-5-week-old plants were infiltrated with LB-grown cultures of *Agrobacterium tumefaciens* strain GV3101 cells transformed with the plasmids of interest as described (Sparkes et al., 2006). Cultures were typically used at an optical density at 600 nm of 1 and mixed in identical proportions for the various combinations. Gene silencing was prevented by co-agroinfiltration with the *A. tumefaciens* strain EHA101 carrying the helper component protease (HCPro) of the watermelon mosaic virus (WMV) in plasmid pGWB702-HCProWMV (the kind gift of Juan José López-Moya and Maria Luisa Domingo-Calap). For pharmacological treatments, stock solutions of mevinolin (MEV), fosmidomycin (FSM) and norflurazon (NF) prepared as described (Llamas et al., 2017; Perello et al., 2014) were diluted in water and 0.05 % Tween 20 right to final concentrations of 10 µM MEV, 200 µM FSM and 20 µM NF. Working solutions were

then infiltrated with a syringe. Infiltration of MEV and FSM was carried out in leaf areas that had been agroinfiltrated with different constructs 24 h earlier. Agroinfiltration of lettuce was performed by vacuum as described (Yamamoto *et al.*, 2018).

Constructs

A truncated version of *Arabidopsis thaliana* HMGR1 (At1g76490) missing the N-terminal 164 aa, referred to as tHMGR (Cankar *et al.*, 2015), was cloned into a pEAQ-USER version of the pEAQ-HT vector kindly provided by George Lomonosoff (Luo *et al.*, 2016; Peyret and Lomonosoff, 2013). Full-length sequences encoding *Pantoea ananatis* crtE, crtB and crtI enzymes were amplified by PCR from plasmid pACCRT-E1B and cloned using the Gateway system into plasmid pDONR207 as described (Majer *et al.*, 2017). Plasmid pGWB506 was used to generate construct 35S:GFP-crtB and plasmid pGWB405 to generate constructs 35S:crtE, 35S:crtE-GFP, 35S:crtB, 35S:crtB-GFP, 35S:crtI and 35S:crtI-GFP (Majer *et al.*, 2017; Nakagawa *et al.*, 2007). Some of these constructs were later used to generate 15-tagged versions by fusing the sequence encoding the first 178 aa residues of the *A. thaliana* HMGR1S isoform to the N-terminal region of the crtE, crtB or crtI enzymes using overlap extension PCR. Plasmid pCA-TXS-His (Besumbes *et al.*, 2004) was used for the expression of a yew (*Taxus baccata*) sequence encoding TXS. Constructs to stimulate lipid body formation (Delatte *et al.*, 2018) were kindly provided by Maria Coca and Tarik Ruiz.

Microscopy

Subcellular localization of GFP-tagged proteins was observed by direct examination of agroinfiltrated leaf tissue at 3 dpi with a Leica TCS SP5 Confocal Laser Scanning Microscope. GFP fluorescence was detected using a BP515-525 filter after excitation at 488 nm, whereas chlorophyll autofluorescence was detected using a LP590 filter after excitation at 568 nm. For light microscopy, leaves were cut into small pieces and cells were separated as described (Lu *et al.*, 2017). Transmission electron microscopy (TEM) of agroinfiltrated leaf areas was performed as described (D'Andrea *et al.*, 2018).

HPLC analysis of pigments

Leaf areas of interest were harvested, snap-frozen in liquid nitrogen and lyophilized until they were completely dry. Approximately 4 mg of this freeze-dried tissue (corresponding to samples from different leaves pooled together) was mixed with 375 μ L of methanol and 25 μ L of a 10 % (w/v) solution of canthaxanthin (Sigma) in chloroform. Extraction and separation of chlorophylls and carotenoids were then performed as described (Emiliani *et al.*, 2018). Eluting compounds were monitored using a photodiode array detector. Peak areas of chlorophylls at 650 nm and carotenoids at 470 nm (lycopene, lutein, β -carotene, violaxanthin, neoxanthin, canthaxanthin) or 280 nm (phytoene) were determined using the Agilent ChemStation software. Quantification was performed by comparison with commercial standards (Sigma).

UV-Vis absorption and resonance Raman

Absorption spectra were measured using a CARY5000 UV/Vis/NIR spectrophotometer (Agilent). Because the analysed tissues were not transparent, we used an integration sphere in reflectance mode, transforming into absorbance using the Kubelka – Munk function (Nobbs, 1985). Resonance Raman spectra were recorded at room temperature and 77 K, the latter with an LN2-flow

cryostat (Air Liquide). Laser excitations at 488, 501.7 and 514.5 nm were obtained with an Ar + Sabre laser (Coherent), and at 577 nm with a Genesis CX STM laser (Coherent). Output laser powers of 10–100 mW were attenuated to <5 mW at the sample. Scattered light was focused into a Jobin-Yvon U1000 double-grating spectrometer (1800 grooves/mm gratings) equipped with a red-sensitive, back-illuminated, LN2-cooled CCD camera. Sample stability and integrity were assessed based on the similarity between the first and last Raman spectra.

Photosynthetic measurements

Photosynthetic efficiencies were assessed by measuring chlorophyll *a* fluorescence with a MAXI-PAM fluorimeter (Heinz Walz GmbH). Photosynthetic parameters were evaluated at 0, 3, 5 and 7 dpi in plants that were previously kept in darkness for at least 30 min to fully open and relax PSII reaction centres. Effective quantum yield of PSII (ϕ PSII) was measured as $(F_m' - F_s)/F_m'$, where F_m' and F_s are the maximum and minimum fluorescence of light-exposed plants, respectively. The chosen light intensity was 21 PAR (AL = 2). Average values were calculated from three biological replicates with three different leaf areas for each replicate.

Antioxidant capacity

Carotenoid extracts prepared as described above were diluted in 400 μ L of diethyl ether and saponified by adding 100 μ L of 10% (w/v) KOH in methanol to avoid interference from chlorophylls. Samples were left shaking for 30 min at 4 $^{\circ}$ C and then diluted with 400 μ L of milliQ water before centrifugation for 5 min at 13 000 rpm and 4 $^{\circ}$ C. The upper phase was collected, dried in a SpeedVac and resuspended in 200 μ L of acetone. Total antioxidant capacity of the mixture was carried out as described (Re *et al.*, 1999).

Bioaccessibility assays

N. benthamiana leaves were either agroinfiltrated with constructs encoding tHMGR, crtE and GFP-crtB (HEB) to produce extrapolastidial phytoene or syringe-infiltrated with a 20 μ M NF solution in water and 0.05 % Tween 20 to accumulate plastidial phytoene by preventing its conversion into downstream carotenoids. Samples from several HEB and NF-treated leaves were collected 5 days after infiltration; non-infiltrated leaves were also collected as controls. Bioaccessibility assays were carried out as described (Estevez-Santiago *et al.*, 2016) using lyophilized tissue samples.

Statistical analyses

Student's *t*-tests were used for statistical analyses using Prism 5.0a (GraphPad) and Office Excel 2010 (Microsoft).

Acknowledgments

We greatly thank Juan José López-Moya, Maria Luisa Domingo-Calap, George Lomonosoff, Maria Coca and Tarik Ruiz for the gift of plasmids, and Christophe Humbert for his help measuring diffuse absorption spectra. This work was funded by the European Regional Development Fund (FEDER) and the Spanish Agencia Estatal de Investigación (grants BIO2017-84041-P and, BIO2017-90877-REDT), Generalitat de Catalunya (2017SGR-710), and European Union's Horizon 2020 (EU-H2020) COST Action CA15136 (EuroCaroten) to MRC. We also acknowledge the financial support of the Severo Ochoa Programme for Centres of Excellence in R&D 2016-2019 (SEV-2015-0533) and the

Generalitat de Catalunya CERCA Programme to CRAG. This work also benefited from the Biophysics Platform of I2BC, supported by iBISA and by the French Infrastructure for Integrated Structural Biology (FRISBI) ANR-10-INBS-05. TBA was funded by a Carlsberg Foundation fellowship. BL is supported by grants from the CSIRO Synthetic Biology Future Science Platform and Macquarie University. LM is supported by La Caixa Foundation PhD INPhINIT (ID 100010434) fellowship LCF/BQ/IN18/11660004, which received funding from the EU-H2020 (MSCA grant 713673). STM is supported by a PhD fellowship from the Spanish Ministry of Education, Culture and Sports (FPU16/04054).

Conflicts of interest

The authors declare no conflict of interest.

Author contributions

T.B.A., B.L., N.C. and M.R.C. designed the research. T.B.A., B.L., L.M., S.T.M., G.B.F., F.A.E., B.O.A., and M.J.L. performed experiments. N.C., B.O.A., M.J.L. and A.A.P. contributed analytic tools; T.B.A., B.L., L.M., S.T.M., G.B.F., F.A.E., B.O.A., A.A.P. and M.R.C. analysed data; T.B.A. and M.R.C. wrote the paper. All authors reviewed and discussed the manuscript.

References

- Alos, E., Rodrigo, M.J. and Zacarias, L. (2016) Manipulation of carotenoid content in plants to improve human health. *Sub-Cell. Biochem.* **79**, 311–343.
- Ampomah-Dwamena, C., Thrimawithana, A.H., Dejnoprat, S., Lewis, D., Easley, R.V. and Allan, A.C. (2019) A kiwifruit (*Actinidia deliciosa*) R2R3-MYB transcription factor modulates chlorophyll and carotenoid accumulation. *New Phytol.* **221**, 309–325.
- Andersen, T.B., Martinez-Swatson, K.A., Rasmussen, S.A., Boughton, B.A., Jorgensen, K., Andersen-Ranberg, J., Nyberg, N. et al. (2017) Localization and in-vivo characterization of *Thapsia garganica* CYP76AE2 indicates a role in Thapsigargin biosynthesis. *Plant Physiol.* **174**, 56–72.
- Avendano-Vazquez, A.O., Cordoba, E., Llamas, E., San Roman, C., Nisar, N., De la Torre, S., Ramos-Vega, M. et al. (2014) An uncharacterized apocarotenoid-derived signal generated in zeta-carotene desaturase mutants regulates leaf development and the expression of chloroplast and nuclear genes in Arabidopsis. *Plant Cell*, **26**, 2524–2537.
- Besumbes, O., Sauret-Gueto, S., Phillips, M.A., Imperial, S., Rodriguez-Concepcion, M. and Boronat, A. (2004) Metabolic engineering of isoprenoid biosynthesis in Arabidopsis for the production of taxadiene, the first committed precursor of Taxol. *Biotechnol. Bioeng.* **88**, 168–175.
- Cankar, K., Jongedijk, E., Klompmaker, M., Majdic, T., Mumm, R., Bouwmeester, H., Bosch, D. et al. (2015) (+)-Valencene production in *Nicotiana benthamiana* is increased by down-regulation of competing pathways. *Biotechnol. J.* **10**, 180–189.
- Cazzonelli, C.I., Hou, X., Alagöz, Y., Rivers, J., Dhami, N., Lee, J., Marri, S. et al. (2020) A cis-carotene derived apocarotenoid regulates etioplast and chloroplast development. *eLife* **9**, e45310.
- Chappell, J., Wolf, F., Proulx, J., Cuellar, R. and Saunders, C. (1995) Is the reaction catalyzed by 3-hydroxy-3-methylglutaryl coenzyme A reductase a rate-limiting step for isoprenoid biosynthesis in plants? *Plant Physiol.* **109**, 1337–1343.
- Cooperstone, J.L., Ralston, R.A., Riedl, K.M., Haufe, T.C., Schweiggert, R.M., King, S.A., Timmers, C.D. et al. (2015) Enhanced bioavailability of lycopene when consumed as cis-isomers from tangerine compared to red tomato juice, a randomized, cross-over clinical trial. *Mol. Nutr. Food Res.* **59**, 658–669.
- D'Amelia, V., Raiola, A., Carputo, D., Filippone, E., Barone, A. and Rigano, M.M. (2019) A basic Helix-Loop-Helix (SIARANCIO), identified from a *Solanum pennellii* introgression line, affects carotenoid accumulation in tomato fruits. *Sci. Rep.* **9**, 3699.
- D'Andrea, L., Simon-Moya, M., Llorente, B., Llamas, E., Marro, M., Loza-Alvarez, P., Li, L. et al. (2018) Interference with Clp protease impairs carotenoid accumulation during tomato fruit ripening. *J. Exp. Bot.* **69**, 1557–1568.
- Delatte, T.L., Scaiola, G., Molenaar, J., de Sousa Farias, K., L. Alves Gomes Albertti, Busscher, J., Verstappen, F. et al. (2018) Engineering storage capacity for volatile sesquiterpenes in *Nicotiana benthamiana* leaves. *Plant Biotechnol. J.* **16**, 1997–2006.
- Diretto, G., Frusciantè, S., Fabbri, C., Schauer, N., Busta, L., Wang, Z., Matas, A.J. et al. (2020) Manipulation of β -carotene levels in tomato fruits results in increased ABA content and extended shelf life. *Plant Biotechnol. J.* **18**, 1185–1199.
- Doblas, V.G., Amorim-Silva, V., Pose, D., Rosado, A., Esteban, A., Arro, M., Azevedo, H. et al. (2013) The SUD1 gene encodes a putative E3 ubiquitin ligase and is a positive regulator of 3-hydroxy-3-methylglutaryl coenzyme A reductase activity in Arabidopsis. *Plant Cell*, **25**, 728–743.
- Domonkos, I., Kis, M., Gombos, Z. and Ughy, B. (2013) Carotenoids, versatile components of oxygenic photosynthesis. *Prog. Lipid Res.* **52**, 539–561.
- Emiliani, J., D'Andrea, L., Ferreyra Lorena Falcone, E., Maulion, E., Rodriguez, E., Rodriguez-Concepcion, M. and Casati, P. (2018) A role for beta, beta-xanthophylls in Arabidopsis UV-B photoprotection. *J. Exp. Bot.* **69**, 4921–4933.
- Esteban, R., Barrutia, O., Artetxe, U., Fernandez-Marin, B., Hernandez, A. and Garcia-Plazaola, J.I. (2015) Internal and external factors affecting photosynthetic pigment composition in plants: a meta-analytical approach. *New Phytol.* **206**, 268–280.
- Estevez-Santiago, R., Olmedilla-Alonso, B. and Fernandez-Jalao, I. (2016) Bioaccessibility of provitamin A carotenoids from fruits: application of a standardised static in vitro digestion method. *Food Funct.* **7**, 1354–1366.
- Ferrero, S., Grados-Torrez, R.E., Leivar, P., Antolin-Llovera, M., Lopez-Iglesias, C., Cortadellas, N., Ferrer, J.C. et al. (2015) Proliferation and morphogenesis of the endoplasmic reticulum driven by the membrane domain of 3-hydroxy-3-methylglutaryl coenzyme A reductase in plant cells. *Plant Physiol.* **168**, 899–914.
- Flores, P., Hernández, V., Hellín, P., Fenoll, J., Cava, J., Mestre, T. and Martínez, V. (2016) Metabolite profile of the tomato dwarf cultivar Micro-Tom and comparative response to saline and nutritional stresses with regard to a commercial cultivar. *J. Sci. Food Agric.* **96**, 1562–1570.
- Harker, M., Holmberg, N., Clayton, J.C., Gibbard, C.L., Wallace, A.D., Rawlins, S., Hellyer, S.A. et al. (2003) Enhancement of seed phytosterol levels by expression of an N-terminal truncated *Hevea brasiliensis* (rubber tree) 3-hydroxy-3-methylglutaryl-CoA reductase. *Plant Biotechnol. J.* **1**, 113–121.
- Hashimoto, H., Uragami, C. and Cogdell, R.J. (2016) Carotenoids and Photosynthesis. *Sub-Cell. Biochem.* **79**, 111–139.
- van Herpen, T.W., Cankar, K., Nogueira, M., Bosch, D., Bouwmeester, H.J. and Beekwilder, J. (2010) *Nicotiana benthamiana* as a production platform for artemisinin precursors. *PLoS One* **5**, e14222.
- Ishigaki, M., Meksjarun, P., Kitahama, Y., Zhang, L., Hashimoto, H., Genkawa, T. and Ozaki, Y. (2017) Unveiling the aggregation of lycopene in vitro and in vivo: UV-Vis, resonance Raman, and Raman imaging studies. *J. Phys. Chem. B* **121**, 8046–8057.
- Koyama, Y. and Fujii, R. (1999) Cis-trans carotenoids in photosynthesis: configurations, excited-state properties and physiological functions. In *The photochemistry of carotenoids* (Frank, H.A., Young, A.J., Britton, G. and Cogdell, R.J., eds), pp. 161–188. Dordrecht, Netherlands: Springer Netherlands.
- Lado, J., Zacarias, L., Gurrea, A., Page, A., Stead, A. and Rodrigo, M.J. (2015) Exploring the diversity in Citrus fruit colouration to decipher the relationship between plastid ultrastructure and carotenoid composition. *Planta*, **242**, 645–661.
- Lee, A.R., Kwon, M., Kang, M.K., Kim, J., Kim, S.U. and Ro, D.K. (2019) Increased sesqui- and triterpene production by co-expression of HMG-CoA reductase and biotin carboxyl carrier protein in tobacco (*Nicotiana benthamiana*). *Metab. Eng.* **52**, 20–28.
- Leivar, P., Antolin-Llovera, M., Ferrero, S., Closa, M., Arro, M., Ferrer, A., Boronat, A. et al. (2011) Multilevel control of Arabidopsis 3-hydroxy-3-methylglutaryl coenzyme A reductase by protein phosphatase 2A. *Plant Cell*, **23**, 1494–1511.
- Llamas, E., Pulido, P. and Rodriguez-Concepcion, M. (2017) Interference with plastome gene expression and Clp protease activity in Arabidopsis triggers a

- chloroplast unfolded protein response to restore protein homeostasis. *PLoS Genet.* **13**, e1007022.
- Llansola-Portoles, M.J., Redeckas, K., Streckaite, S., Illoia, C., Pascal, A.A., Telfer, A., Vengris, M. et al. (2018) Lycopene crystalloids exhibit singlet exciton fission in tomatoes. *Phys. Chem. Chem. Phys.* **20**, 8640–8646.
- Llorente, B., D'Andrea, L., Ruiz-Sola, M.A., Botterweg, E., Pulido, P., Andilla, J., Loza-Alvarez, P. et al. (2016) Tomato fruit carotenoid biosynthesis is adjusted to actual ripening progression by a light-dependent mechanism. *Plant J.* **85**, 107–119.
- Llorente, B., Torres-Montilla, S., Morelli, L., Florez-Sarasa, I., Matus, J.T., Ezquerro, M., D'Andrea, L. et al. (2020) Synthetic conversion of leaf chloroplasts into carotenoid-rich plastids reveals mechanistic basis of natural chromoplast development. *Proc. Natl Acad Sci USA*, **117**, 21796–21803.
- Lomonosoff, G.P. and D'Aoust, M.A. (2016) Plant-produced biopharmaceuticals: a case of technical developments driving clinical deployment. *Science*, **353**, 1237–1240.
- Lu, Y., Stegemann, S., Agrawal, S., Karcher, D., Ruf, S. and Bock, R. (2017) Horizontal transfer of a synthetic metabolic pathway between plant species. *Curr. Biol.* **27**, 3034–3041.e3033.
- Luo, D., Callari, R., Hamberger, B., Wubshet, S.G., Nielsen, M.T., Andersen-Ranberg, J., Hallstrom, B.M. et al. (2016) Oxidation and cyclization of casbene in the biosynthesis of Euphorbia factors from mature seeds of *Euphorbia lathyris* L. *Proc. Natl Acad. Sci. USA*, **113**, E5082–5089.
- Majer, E., Llorente, B., Rodriguez-Concepcion, M. and Daros, J.A. (2017) Rewiring carotenoid biosynthesis in plants using a viral vector. *Sci. Rep.* **7**, 41645.
- Mapelli-Brahm, P., Desmarchelier, C., Margier, M., Reboul, E., Melendez-Martinez, A.J. and Borel, P. (2018) Phytoene and phytofluene isolated from a tomato extract are readily incorporated in mixed micelles and absorbed by caco-2 cells, as compared to lycopene, and SR-BI is involved in their cellular uptake. *Mol. Nutr. Food Res.* **62**, e1800703.
- Massaretto, I.L., Albaladejo, I., Purgatto, E., Flores, F.B., Plasencia, F., Egea-Fernández, J.M., Bolarin, M.C. et al. (2018) Recovering tomato landraces to simultaneously improve fruit yield and nutritional quality against salt stress. *Front Plant Sci.* **9**, 1778.
- Melendez-Martinez, A.J., Mapelli-Brahm, P., Benitez-Gonzalez, A. and Stinco, C.M. (2015) A comprehensive review on the colorless carotenoids phytoene and phytofluene. *Arch. Biochem. Biophys.* **572**, 188–200.
- Melendez-Martinez, A.J., Mapelli-Brahm, P. and Stinco, C.M. (2018) The colourless carotenoids phytoene and phytofluene: from dietary sources to their usefulness for the functional foods and nutraceuticals industries. *J. Food Compos. Anal.* **67**, 91–103.
- Mou, B. (2009) Nutrient content of lettuce and its improvement. *Curr. Nutr. Food Sci.* **5**, 242–248.
- Müller, L., Fröhlich, K. and Böhm, V. (2011) Comparative antioxidant activities of carotenoids measured by ferric reducing antioxidant power (FRAP), ABTS bleaching assay (α TEAC), DPPH assay and peroxy radical scavenging assay. *Food Chem.* **129**, 139–148.
- Nakagawa, T., Suzuki, T., Murata, S., Nakamura, S., Hino, T., Maeo, K., Tabata, R. et al. (2007) Improved Gateway binary vectors: high-performance vectors for creation of fusion constructs in transgenic analysis of plants. *Biosci. Biotechnol. Biochem.* **71**, 2095–2100.
- Nobbs, J.H. (1985) Kubelka-munk theory and the prediction of reflectance. *Prog. Color. Relat. Top.* **15**, 66–75.
- Nogueira, M., Enfissi, E.M.A., Welsch, R., Beyer, P., Zurbruggen, M.D. and Fraser, P.D. (2019) Construction of a fusion enzyme for astaxanthin formation and its characterisation in microbial and plant hosts: A new tool for engineering ketocarotenoids. *Metab. Eng.* **52**, 243–252.
- Nogueira, M., Mora, L., Enfissi, E.M., Bramley, P.M. and Fraser, P.D. (2013) Subchromoplast sequestration of carotenoids affects regulatory mechanisms in tomato lines expressing different carotenoid gene combinations. *Plant Cell*, **25**, 4560–4579.
- Pankratov, I., McQuinn, R., Schwartz, J., Bar, E., Fei, Z., Lewinsohn, E., Zamir, D. et al. (2016) Fruit carotenoid-deficient mutants in tomato reveal a function of the plastidial isopentenyl diphosphate isomerase (IDI1) in carotenoid biosynthesis. *Plant J.* **88**, 82–94.
- Perello, C., Rodriguez-Concepcion, M. and Pulido, P. (2014) Quantification of plant resistance to isoprenoid biosynthesis inhibitors. *Methods Mol. Biol.* **1153**, 273–283.
- Peyret, H. and Lomonosoff, G.P. (2013) The pEAQ vector series: the easy and quick way to produce recombinant proteins in plants. *Plant Mol. Biol.* **83**, 51–58.
- Pollier, J., Moses, T., Gonzalez-Guzman, M., De Geyter, N., Lippens, S., Vanden Bossche, R., Marhavy, P. et al. (2013) The protein quality control system manages plant defence compound synthesis. *Nature*, **504**, 148–152.
- Ravanello, M.P., Ke, D., Alvarez, J., Huang, B. and Shewmaker, C.K. (2003) Coordinate expression of multiple bacterial carotenoid genes in canola leading to altered carotenoid production. *Metab. Eng.* **5**, 255–263.
- Re, R., Pellegrini, N., Prottogente, A., Pannala, A., Yang, M. and Rice-Evans, C. (1999) Antioxidant activity applying an improved ABTS radical cation decolorization assay. *Free Radic. Biol. Med.* **26**, 1231–1237.
- Robert, B. (1999) The electronic structure, stereochemistry and resonance Raman spectroscopy of carotenoids. In *The Photochemistry of Carotenoids* (Frank, H.A., Young, A.J., Britton, G. and Cogdell, R.J., eds), pp. 189–201. Dordrecht, Netherlands: Springer Netherlands.
- Rodriguez-Concepcion, M., Avalos, J., Bonet, M.L., Boronat, A., Gomez-Gomez, L., Hornero-Mendez, D., Limon, M.C. et al. (2018) A global perspective on carotenoids: Metabolism, biotechnology, and benefits for nutrition and health. *Prog. Lipid Res.* **70**, 62–93.
- Rodriguez-Concepcion, M. and Boronat, A. (2015) Breaking new ground in the regulation of the early steps of plant isoprenoid biosynthesis. *Curr. Opin. Plant Biol.* **25**, 17–22.
- Ruiz-Sola, M.A., Barja, M.V., Manzano, D., Llorente, B., Schipper, B., Beekwilder, J. and Rodriguez-Concepcion, M. (2016) A single arabidopsis gene encodes two differentially targeted geranylgeranyl diphosphate synthase isoforms. *Plant Physiol.* **172**, 1393–1402.
- Sadali, N.M., Sowden, R.G., Ling, Q. and Jarvis, R.P. (2019) Differentiation of chromoplasts and other plastids in plants. *Plant Cell Rep.* **38**, 803–818.
- Schwach, F., Vaistij, F.E., Jones, L. and Baulcombe, D.C. (2005) An RNA-dependent RNA polymerase prevents meristem invasion by potato virus X and is required for the activity but not the production of a systemic silencing signal. *Plant Physiol.* **138**, 1842–1852.
- Sparkes, I.A., Runions, J., Kearns, A. and Hawes, C. (2006) Rapid, transient expression of fluorescent fusion proteins in tobacco plants and generation of stably transformed plants. *Nat. Protoc.* **1**, 2019–2025.
- Sun, T., Yuan, H., Cao, H., Yazdani, M., Tadmor, Y. and Li, L. (2018) Carotenoid metabolism in plants: the role of plastids. *Mol. Plant*, **11**, 58–74.
- Suzuki, M., Takahashi, S., Kondo, T., Dohra, H., Ito, Y., Kiriiwa, Y., Hayashi, M., et al. (2015) Plastid Proteomic Analysis in Tomato Fruit Development. *PLoS One* **10**, e0137266. <https://doi.org/10.1371/journal.pone.0137266>.
- Tamary, E., Nevo, R., Naveh, L., Levin-Zaidman, S., Kiss, V., Savidor, A., Levin, Y. et al. (2019) Chlorophyll catabolism precedes changes in chloroplast structure and proteome during leaf senescence. *Plant Direct*, **3**, e00127.
- Wang, Z., Xu, W., Kang, J., Li, M., Huang, J., Ke, Q., Kim, H.S. et al. (2018) Overexpression of alfalfa Orange gene in tobacco enhances carotenoid accumulation and tolerance to multiple abiotic stresses. *Plant Physiol. Biochem.* **130**, 613–622.
- Wu, S., Schalk, M., Clark, A., Miles, R.B., Coates, R. and Chappell, J. (2006) Redirection of cytosolic or plastidial isoprenoid precursors elevates terpene production in plants. *Nat. Biotechnol.* **24**, 1441–1447.
- Yamamoto, T., Hoshikawa, K., Ezura, K., Okazawa, R., Fujita, S., Takaoka, M., Mason, H.S. et al. (2018) Improvement of the transient expression system for production of recombinant proteins in plants. *Sci. Rep.* **8**, 4755.
- Yin, J.L. and Wong, W.S. (2019) Production of santalenes and bergamotene in *Nicotiana tabacum* plants. *PLoS One*, **14**, e0203249.
- Zheng, X., Giuliano, G. and Al-Babili, S. (2020) Carotenoid biofortification in crop plants: citius, altius, fortius. *Biochim. Biophys Acta Mol. Cell Biol. Lipids*, **1865**, 158664.